Research Article

Current Research in Statistics & Mathematics

The Ulianov Sphere Network - A Digital Model for Representation of Non-Euclidean Spaces

Policarpo Yōshin Ulianov*

***Corresponding Author**
Policarpo Yōshin Ulianov

Submitted: 2023, Sep 07; **Accepted**: 2023, Oct 02; **Published**: 2023, Oct 11

Citations: Ulianov, P. Y. (2023). The Ulianov Sphere Network - A Digital Model for Representation of Non-Euclidean Spaces. *Curr Res Stat Math, 2*(1), 42-55.

Abstract

This article introduces a new model for the non-Euclidean spaces' representation, in which the coordinates and distances are considered as digital nature. This model, called the Ulianov Sphere Network (USN), presents a new way for visualizing the curved spaces, such as those defined in the context of the General Relativity Theory (GRT).

The USN model has the potential to facilitate the calculation procedures concerning the problems handled by the GRT, since it relies on a very simple mathematical formulation, which can be easily implemented in numerical computing systems.

The proposed model is a mathematical tool that facilitates the manipulation of non-Euclidean spaces, for the simple expedient of constructing over a continuous plain space, a network of hyperspheres that behaves as a non-Euclidean digital space.

Initially, the USN model has no real connection with the observed physics in our universe, being basically a theoretical abstraction. However, as will be shown in this article, the application of the UNS model allows inferring some formulas related to the GRT and also with Newton's Law of Gravitation. Thus, the hypothesis that the USN model is actually somehow related to the physical basis of operation in our universe is not discarded.

1. Introduction

About 300 years before Christ, the Greek philosopher Euclid organized geometric knowledge in a formal system, called Euclidean geometry, by defining a series of entities (point, line, plane, etc...) within a set of postulates, for example, that the sum of internal angles of a triangle is always equal to 180 degrees [1].

The universal validity of Euclidean geometry began to be questioned in the 18th century by the Italian mathematician Sacchieri but it was only in the 19th century that some mathematicians, like the German Gauss the Russian Lobachevsky and the Hungarian Bolyai who envisioned the possibility that alternative (non-Euclidean) geometries could also be valid [2-5].

In the twentieth century, several works such as Riemann's and Poincare´s formalized postulates applicable to non-flat spaces, thereby generating a series of non-Euclidean geometry.

These geometries are no longer mere mathematical curiosity with Einstein's publication of the General Relativity Theory, ***of which the*** mathematical basis was given by the Italian mathematician Tullio Levi-Civita, who defined the Tensor calculus which is based on manipulation of non-Euclidean geometries [6-9].

In the GRT, Einstein unified space and time in a four-dimensional continuum, which is modeled as a Minkowski space and which curvature will depend on the content of matter-energy in the considered space [10].

Therefore, in the context of the GRT, phenomena related to matter, such as the planet's orbits, are no longer explained by interactions among the gravitational forces and begin to be interpreted as geodesic paths (the shortest trajectory between two points) within the Minkowski space [11].

The main equation of the GRT is based on two tensors: The Einstein Tensor ($\mathbf{G}_{\mu\nu}$) which is related to the curvature of space-time and the Energy-momentum Tensor ($\mathbf{T}_{\mu\nu}$) which depends on the distribution of matter and energy. This equation is defined as:

$$\mathbf{G}_{\mu\nu} = -\frac{8\pi G}{c^2}\mathbf{T}_{\mu\nu} \tag{1}$$

Where G is the gravitational constant and c is the speed of the light. In a space without matter-energy, the space time coordinates (ct,x,y,z) are related to a flat space where the Einstein Tensor is:

$$g_{\mu\nu} = \begin{bmatrix} 1 & 0 & 0 & 0 \\ 0 & -1 & 0 & 0 \\ 0 & 0 & -1 & 0 \\ 0 & 0 & 0 & -1 \end{bmatrix} \tag{2}$$

In this case, a metric of a flat Minkowski space is:

$$ds^2 = c^2dt^2 - dx^2 - dy^2 - dz^2 \qquad (3)$$

In the presence of matter-energy, the Einstein Tensor can be defined as:

$$\mathbf{G}_{\mu\nu} = \mathbf{R}_{\mu\nu} - \frac{1}{2} R\, g_{\mu\nu} = -\frac{8\pi G}{c^2}\mathbf{T}_{\mu\nu} \qquad (4)$$

Where $\mathbf{R}_{\mu\nu}$ is the Ricci tensor and   is a scalar of curvature.

From equation (4) the GRT field equations can be assembled, resulting in a series of partial differential nonlinear equations of second order and with hyperbolic elliptical coupling.

These equations are usually not very easy to be solved, even for the simplest cases, and for more complex cases the solution involves the use of numerical simulations.

In the basic case, where there is a single spherical body of mass M in an empty space, the resolution of the equation (4) generates a solution called the Schwarzschild metric [12].

This metric can be defined in spherical coordinates by the following equation:

$$ds^2 = c^2\left(1 - \frac{2GM}{c^2 r}\right)dt^2 - \frac{dr^2}{1 - \frac{2GM}{c^2 r}} - r^2 d\Omega^2 \qquad (5)$$

Where $d\Omega^2$ is defined by:

$$d\Omega^2 = d\theta^2 + \sin^2(\theta)\, d\phi^2 \qquad (6)$$

Where (r, θ, ϕ) indicates the considered point from a spherical coordinate system, whose center is positioned at thegravity center of the considered spherical body.
For M equal to zero, the equation (5) relapses into the Minkowskian metric for a flat space generating the equation (3), which can also be written in spherical coordinates, as follows:

$$ds^2 = c^2dt^2 - dr^2 - r^2 d\Omega^2 \qquad (7)$$

For M values greater than zero, there will be an r value (the Schwarzschild radius) for which the value that multiplies dr^2 tends to the infinite, while the value that multiplies dt^2 tends to zero:

$$r_s = \frac{2GM}{c^2} \qquad (8)$$

Since equation (5) is valid only for the space outside the considered spherical body, if the radius of the body is greater than the Schwarzschild radius a division by zero in equation (5) will be avoided. In cases where the body radius is less than the Schwarzschild radius, there will be a situation in which the space curvature is so pronounced that not even the light can overcome it, creating an object called a black hole [13].

If the body has neither electric charge nor spin, the value of the Schwarzschild radius will define the events horizon of the black hole.

It is interesting to notice that the solution of equation (4) is quite complex and even Einstein only published the solution to the simplest case (space without matter and energy).The solution to the case of a single spherical body, presented in equations (5) and (6), was only obtained by the physicist Karl Schwarzschild about a year after Einstein had published the equation (4) in the context of the GRT.

2. Traditional view of the space-time curvature

The contraction of space-time caused by the presence of matter-energy is somewhat difficult to visualize, particularly considering that time is also curved. Therefore, even the simplest case represented by equation (5), where a single body distorts the space, can hardly be viewed in its full four-dimensional form.

A simple analogy, which facilitates the understanding of space contraction is to consider only two dimensions of space. Figure 1 shows the case of an elastic network (represented by black lines) that is distorted by the presence of mass in a spherical body (represented in blue).

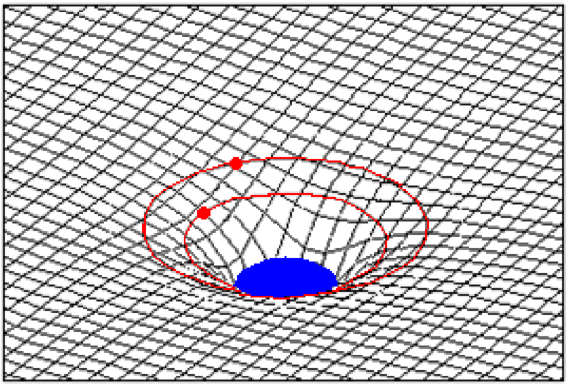

Figure 1: Spherical body bending an elastic network.

In Figure 1, the two red circles represent geodesic trajectories followed by bodies of negligible mass (represented in red). If these bodies are moved with no friction on a flat space in a uniform rectilinear motion, its geodesic trajectory will be by a straight line. As for the case of the curved space shown in Figure 1, the geodesic trajectory will take the shape of a circle or more generally the shape of an ellipse.

Despite the elastic network's analogy being somewhat grossly simplified, it shows how planets orbiting around a star can assume circular paths, based solely on the space-time curvature without adding any gravitational force which acts at distance. One of the failures in the analogy shown in Figure 1 is that some of the "houses" in the elastic network, if near to the central mass, become larger. This is because these homes "sink" into a third dimension that does not actually exist (because the model used is a two-dimensional space).

In a more realistic representation, shown in Figure 2, it is observed that all "homes" defined in a two-dimensional curved space, in fact shrink and approach to the point occupied by the mass.

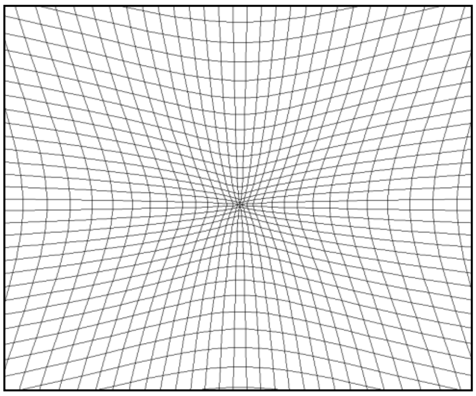

Figure 2: Curvature in a two-dimensional space.

3. Digital representation of an Euclidean space

In this section we will start presetting the USN model, approaching at first a simple representation of a flat space, in which both space and time are defined in a digital form. This means there will be a minimum distance in time and space, which cannot be subdivided. Thus, any considered displacement will always be set as a integer value that multiplies a minimum distance of time or space.

In practice, these minimum distance values can be associated with a unitary scale based on the Planck distance (1.616 x 10^{-35}m) and in the Planck time (5.391 x 10^{-44}s) [14]. As the value of Planck distance is extremely small, the representation in meters of an integer number of Planck distances generates a value with precision of up to 35 digits after point, which in practice can be considered as a real number.

A simple two-dimensional digital space can be defined based on a chess board with squares set on a real plan (*x,y*), as shown in Figure 3.

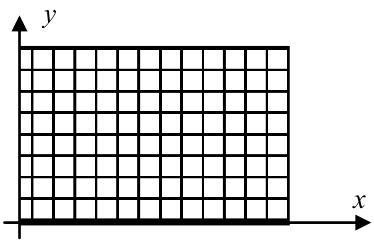

Figure 3: Board forming a digital space

Considering that each house of this board has a unitary size (ℓ_μ), a digital space composed of two integers coordinates (*Nx,Ny*) can be defined, which relate to the real plan (*x,y*) by the following equations:

$$x(Nx) = (Nx \pm 0.5)\,\ell_u$$
$$y(Ny) = (Ny \pm 0.5)\,\ell_u \qquad (9)$$

Where the term ± 0.5 ℓ_μ indicates a positioning uncertainty inherent to any considered digital space. The representation of Figure 3, however, is flawed in the sense it generates two preferential directions given by the rectangular shape of the squares sets and imposing a fixed direction for the axes (*x,y*) .

Circular units should be used in a more realistic representation, as shown in Figure 4, where the axes defining the coordinate system may take any position.

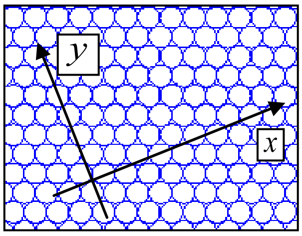

Figure 4: Board with circular units.

For the digital space shown in Figure 4, a digital time can be defined by using a series of overlapped boards, as shown in Figure 5.

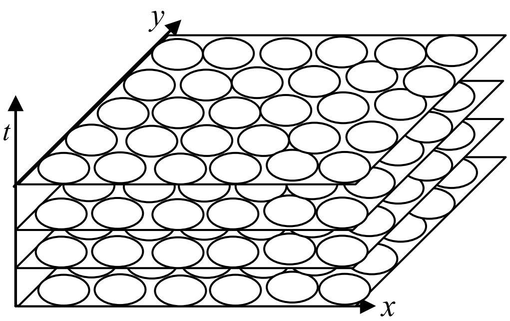

Figure 5: Time definition through boards overlapping.

In this model, it can be defined a point-like particle that occupies a certain position on the board and moves by “jumping” one house at a time, similar to a “king” moving on a chessboard.

In Figure 6, in order to facilitate viewing, the three-dimensional board which has been shown in Figure 5 is divided into "time frames", shown in sequence. This is an analogous representation to a movie pellicle where individual “slides” sequences will compose the film.

Two particles represented by blue and red circles can be seen in Figure 6. Although the particles are always at rest in each frame, in the frames sequence it can be observed that the red particle moves at unitary speed while the blue particle always occupies the same position.

This aspect is also seen in a movie pellicle, where each frame itself contains only static objects and the sense of movement and speed comes only when the frames are observed in sequence.

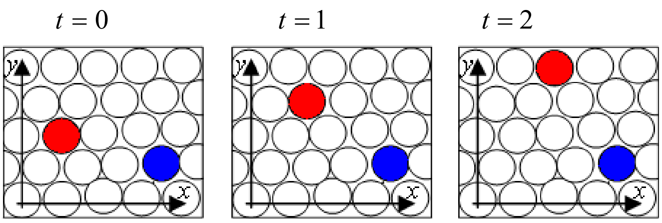

Figure 6: Point-like particles in a digital space-time.

In a more realistic representation,, the circular houses in Figure 6 can be conceived as spheres, defined over a three-dimensional space, like ping pong balls piled up in a rectangular box.

In this case a balls layer at the bottom of the box will define a two-dimensional board for a given time. Inclusion of new balls will grow the pile generating overlapped boards in a similar way to what was presented in Figure 5. But in this case an "inclined" plan inside the box can be defined, where the dimensions of space and time cease to be clearly distinct, creating a unique space-time entity.

In the models presented in Figures 4 and 5, two-dimensional spaces were considered in order to facilitate viewing.

A more complete model should consider a three-dimensional space and also time. In this case, for a complete space-time representation, it must be considered a set (a network) of hyperspheres (spheres of four dimensions) Any house within this network can be defined by counting the hyperspheres in relation to a system of four orthogonal axes. This representation implies in a set of four integers coordinates (*Nt,Nx,Ny,Nz*).

By multiplying each one of these coordinated by the Planck distance, we can define a space-time as a function of four coordinates (*ct,x,y,z*) that in practice can be treated as real numbers.

By using a scale where the speed of light and the Planck distance and Planck time assume unitary values, we can define a network of hyperspheres whose diameters are also unitary. Thus, the center of each hypersphere will be positioned in a uniform grid defined over a continuous space, as shown in Figure 7. In this figure it is displayed once more a two-dimensional case, which can also be seen as a cut in four-dimensional network, where the values of other coordinates are fixed.

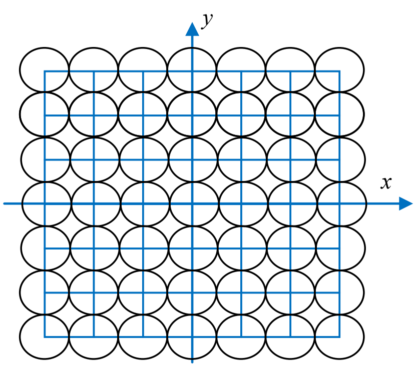

Figure7: Positioning of a uniform network of spheres over a two-dimensional space.

The network of spheres shown in Figure 7, seems to be defined in terms of a certain orientation of axes. However, in a digital representation, there will be an uncertainty in the positioning, which results in some overlap of adjacent hyperspheres.

Considering this uncertainty, we obtain a representation as shown in Figure 8, where a preferential spatial orientation ceases to exist.

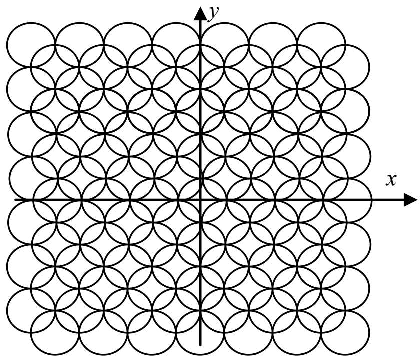

Figure 8: Uncertainty of positioning of a two-dimensional spheres network.

4. Digital representation of a non-Euclidean space

In order to define a digital representation of a non-Euclidean space in the USN model, should be introduced a special type of hypersphere, called Ulianov Sphere (usphere). An usphere can be defined accordingly to the following properties:

- An usphere consists of a spherical surface of null thickness (spherical shell) defined over a continuous four-dimensional Euclidean space;
- An usphere is completely defined by a center point and by a given radius (or diameter);
- The diameter of an usphere always takes a real value greater or equal to one unit (defined in the Planck unitary system);
- Undergoing an usphere to a positive radial force field, as shown in Figure 9, its radius tends to increase in proportion to the intensity of the applied field;
- Undergoing an usphere of unitary diameter to an unitary radial negative force field, as shown in Figure 10, it is collapsed (the diameter becomes null). In this condition the usphere becomes an Ulianov Hole (uhole). If the force field is removed, the uhole expands generating again an usphere of unitary diameter.

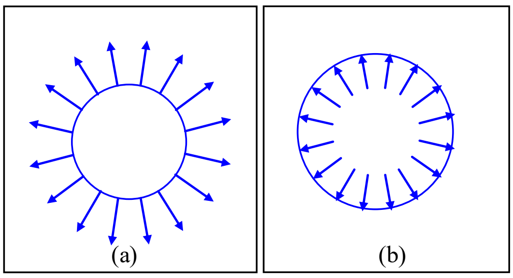

Figure 9:
a) Usphere subjected to a positive radial force field.
b) Usphere with increased radius.

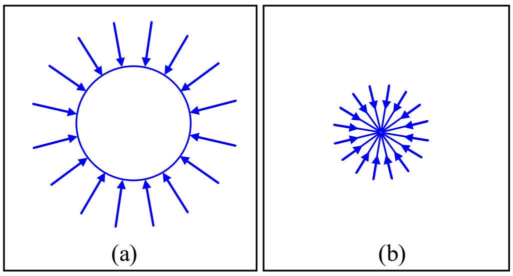

Figure 10:
a) Usphere subjected to a negative radial force field
b) Usphere collapsed becomes uhole.

By observing Figures 9 and 10 we can affirm that in an equilibrium condition, with no force being applied, the diameter of an usphere will always be unitary.

An uhole exists only while a force field is compressing it. At the time when this field is eliminated, the uhole expands and becomes an usphere.

Another important property of an usphere is its surface formed by the aligning of a large number of uholes, tending to the infinite. Thus if an usphere is placed in an empty space, then some uholes that form it will tend to expand until they occupy all available spaces.

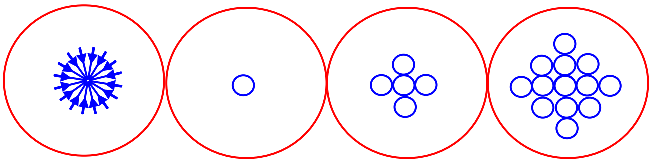

Figure 11: Generation of an usphere Network.

This process is shown in Figure 11, initially there is a single uhole being compressed by a force field. When this field is removed, there is initially a single usphere. Then, some uholes forming the surface of the original usphere also expand, generating new uspheres and so on.

The final formed structure takes the form of a hyperspheres network, which was called Ulianov Sphere Network (USN).

An USN is originated from a single compressed uhole, as shown in Figure 11 and it expands until filling all the available spaces. When an USN ceases expanding, each one of the infinite uholes composing it will be submitted to an unitary radial negative force field, because otherwise the USN would still be expanding. This generates an infinite tension on the USN, which will cause each usphere to touch its neighbors forming a compact network with no empty areas.

It is important to notice in Figure 11 that the USN own evolution in time is shown within red circles that represent sequences of uspheres expanding in time. Thus, a complete USN will have four dimensions, three related to space and one related to time.
Usually, an USN will expand occupying the entire available volume in the spatial dimensions and will tend to grow continuously in the time dimension.

In a uniform USN, there will be a similar organization to that shown in Figure 7, in which all the uspheres have unitary diameter.

Starting from a uniform USN, if we apply a force field inside an usphere, this usphere will be compressed, generating an uhole. However, this new uhole is different from all other uholes (which form the walls of the existing uspheres) because the force field that created it, generates a reaction field that acts on the USN tending to expand all existing uspheres inside it.

This special type of uhole was called Ulianov Dynamic Hole (udyhole).

The neighboring uspheres to the formed udyhole will tend to expand further, as shown in Figure 12, in which a red dot indicates the location where three uspheres were compressed at one same point generating three overlapping udyholes. We can also consider that the overlapping of several udyholes on the same point generates a single udyhole, which is "bigger" only in the direction where it distorts more the uspheres which are its neighbors.

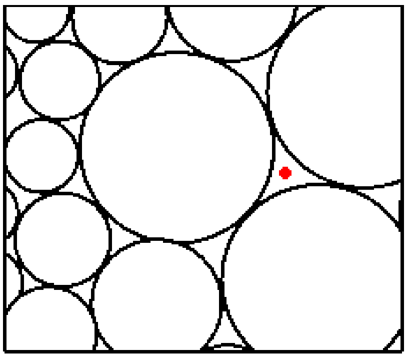

Figure 12: Ulianov Sphere Network distortion caused by the compression of some uspheres.

A udyhole has characteristics of a point-like particle and can move around on the network, "jumping" from one to another usphere. Thus, an udyhole moves in digital space-time defined by the USN, always jumping a house at a time.

On this way, for each new unitary time (Planck time) a given udyhole can stand still or move a unitary distance (Planck distance). Therefore, the udyhole speed will always be zero or equal to the speed of light.

The Udyhole movement can also be associated to the movement of the force field that defines it. Thus, we can consider the udyhole not actually moving, but the force field passing from an usphere to another, and so the abandoned house “inflates" while the new house occupied by the field gets "empty".

An important observation is that an udyhole always moves a "house" at a time, regardless of the effective usphere diameter that will be occupied next. Thus, from the point of view of an udyhole, an USR will be uniform with all network uspheres always having unitary size.

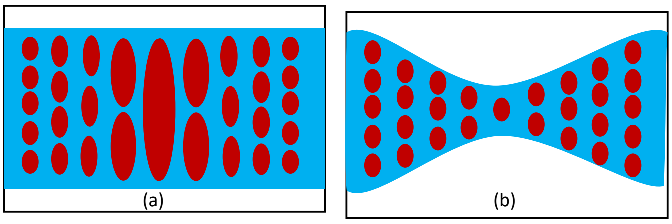

Figure 13: Analogy of a river crossed by rows of stones. In (a) the actual width is observed and (b) the number of leaps.

This aspect is illustrated at the analogy shown in Figure 13, in which a uniform width river is crossed by a series of stones of different sizes. Suppose now that a frog will cross the river, passing from one stone to another with only one jump (regardless of the stone size). For this frog, the river has no longer a constant width being narrower on the central point and becoming wider at the edges. Thus, for the frog, it seems like all the stones of the river had the same size, as shown in Figure 13-b.

Therefore, we can use the motion of a udyholes to define a digital metric, in which the distance between two given points can be measured by counting the number of spheres that the udyhole should "jump" to go from one point to another, considering a path defined by a straight line in real space that contains the network.

Thus, in the USN model there will always exist two representations of distance, a "real metric" given as a function of space containing the network and other "digital metric" given by the counting of the number of spheres, regardless of the size of each one of them. For a uniform network, these two metrics will be identical, but in the presence of udyholes distorting the network, the two metrics become quite distinct.

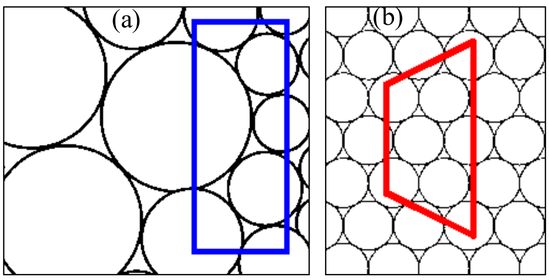

Figure 14:
a) Usphere network seen by a real metric.
b) Usphere network seen by a digital metric.

Figure 14 illustrates a simple case of application of these two metrics over a distorted network. We observe in Figure 14-a, the network from the point of view of real metric, in which the square in blue represents the displacement of an udyhole accordingly to a rectangular trajectory. Figure 14-b, in turn, displays the same network accordingly to the digital metric. In this case, the displacement of the udyhole is represented by a red trapezoid, whose internal angles are equal to 90 degrees. Thus although the real metric is always Euclidean, the digital metric, for a distorted network, will typically be associated with a non-Euclidean space.

Figure 15 illustrates a case where an USN is strongly distorted due to the presence of a large number of udyholes placed at its center. The grid drawn in this figure illustrates the observed distance accordingly to the digital metric, and the real metric is shown in two points with the aid of the red circles observed in the figure. Notice that there is a similar grid between the lines represented in Figure 15 and the river margin represented in Figure 13. In terms of a real metric, these lines are parallel and form a uniform grid, while in the digital metric, the lines bend towards the figure center. Therefore, in both representations the angles among all the lines that intersect to form the grid are always equal to 90 degrees. Moreover, in digital metric, despite the grid lines are curved they still represent the shortest distance between two points on its edges, which indicates that these curved lines represent geodesic trajectories.

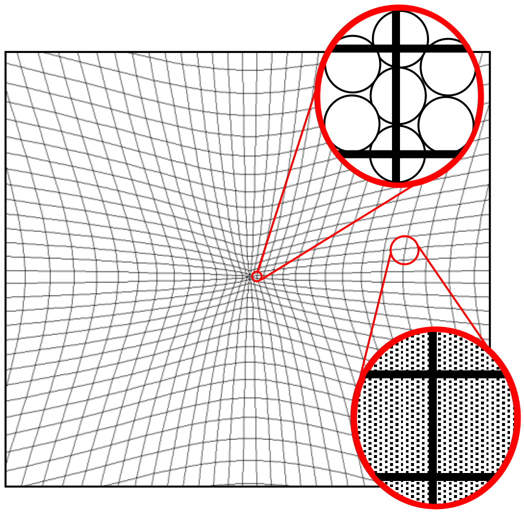

Figure 15: USN with a big distortion in its central point on which was drawn a uniform grid.

If we compare Figure 2 as defined in the context of GRT with Figure 15 defined in the USN model, we can observe the effect of an accumulation of udyholes at the center of a uniform usphere network is similar to that obtained by the accumulation of mass at the center of an empty space. Thus, we can associate udyholes to a unitary value of mass (K_{mu}), and so the association of N unitary udyholes at one point generates a new udaynahole with mass M that is equal to NK_{mu}.

On this way, if a certain amount of mass is associated to udyholes, the results obtained in the USN model will be very similar to those obtained by the GRT, but using a much more trivial mathematics.

However, it is important to note that the USN model and the GRT operate accordingly to opposite premises. It occurs because the GRT considers the presence of mass that "shrinks" the space while the USN model considers that the presence of mass (udyholes) actually "expands" the space.

5. Calculation of the Schwarzschild Metric

In order to validate the USN model, it will be used in this section for a simple case in which a spherical body of mass M is positioned in an empty space and a solution similar to the equation for the Schwarzschild metric (presented in equation 5) must be obtained.

Initially we can define a flat continuum space-time, in which a point is represented by four real coordinates:

$$P_r = (a_1, a_2, a_3, a_4) \qquad (10)$$

On this space we will initially define a uniform USN, composed of uspheres with radius equal to r_0. On this network we can define an orthogonal system composed by four Cartesian axes that locates a given usphere within the network from four integers coordinates:

$$P_I = (N_t, N_x, N_y, N_z) \qquad (11)$$

Over this digital space we can define a Minkowski space, presented in equation (3), multiplying the space coordinates by the Planck distance defined by the parameter ℓ_{p} :

$$(c\,t, x, y, z) = (\ell_{\mathrm{p}} N_t, \ell_{\mathrm{p}}\, N_x, \ell_{\mathrm{p}}\, N_y, \ell_{\mathrm{p}}\, N_z) \qquad (12)$$

Considering that the USN is uniform, the center of each usphere can be located as follows:

$$(a_1, a_2, a_3, a_4) = (2r_0 N_t, 2r_0 N_x, 2r_0 N_y, 2r_0 N_z) \qquad (13)$$

Now consider a line of Uspheres leaving the origin towards any direction of the space. On this line an axis will be defined in which a distance d, in relation to the origin (real metric), is associated to a count of spheres N_d (digital metric).Applying a unitary radial force field in a single usphere in the center of the considered space, it will be compressed, becoming an udyhole, as shown in Figure 16.

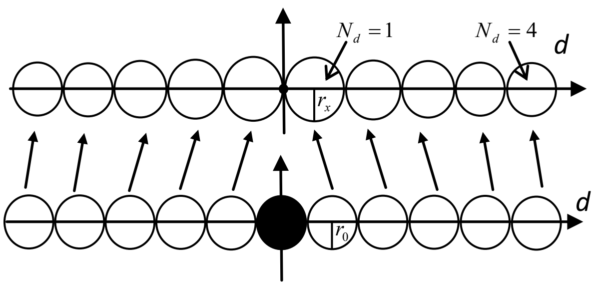

Figure 16: Usphere network with an udyhole being formed.

We can see in Figure 16, the collapse of the black sphere moves the nearby spheres and slightly increases their sizes. The farther from the udyhole is the considered sphere, smaller its radius increase will be.

Considering only values greater than zero for N_d, we can show the considered radius in the line, after compression of the central usphere will assume the following value:

$$r_x(N_d) = r_0\left(1 + \frac{1}{N_d(N_d+1)}\right) \qquad (14)$$

Since for the equation (14) the sum of value added to the radius of each sphere is given by:

$$\sum_{N_d=1}^{N_d=\infty} \frac{r_0}{N_d(N_d+1)} = r_0 \qquad (15)$$

Thus, equation (14) generates an increase in the uspheres radius whose sum is exactly equal to the space generated by the compression of the central usphere. On this way, the total volume occupied by the USR remains constant.Despite the above premise being fairly obvious, there are actually two basic possible considerations when a usphere in a USR is compressed, generating an udyhole:

• The total USN volume does not change - In this case the volume generated by compression is equal to the volume increase in the other uspheres and the equations (14) and (15) are valid. Within this consideration we can deduce the formula of Newton's gravitation law, which will be more detailed in the next section;

• The total USN volume increases - In this case the volume increase in all uspheres is greater than the usphere volume that was compressed and so the equations (14) and (15) become invalid. Within this consideration we can deduce compatible formulas with the GRT, which will be seen next.

In order to define a new equation modeling the increase in radius of each usphere, we initially must calculate the increase in the final volume in the distorted USN. However, this increase will vary in function of space's characteristics in which the USN is defined.

Thus, we will build on a specific case (considering only the USN spatial dimensions) in which a three-dimensional USN is contained on the surface of a hypersphere of four dimensions.
Under these conditions, the USN will occupy all available volume on the surface of the hypersphere. In this case, the USN volume can also be associated to the volume contained within a three-dimensional sphere defined in a flat space.

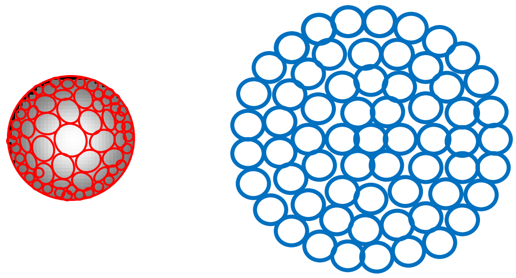

Figure 17: Two-dimensional usphere network defined on the surface of a sphere (in red) and flattened on a circular area (in blue) equivalent to the spherical surface area.

In order to facilitate the visualization of this model, we initially consider an analogous case shown in Figure 17 in which a two-dimensional usphere network (represented in red) is defined on a sphere surface. This two-dimensional network can also be

defined on a flat surface, creating an equivalent circular area, shown in blue in Figure 17.
Notice both representations, shown in Figure 17, are quite equivalent for the uspheres in the network center, but at the flattened network there will be an "edge" that does not really exist in the original spherical surface.

Now, consider the case of the three-dimensional USN, analogous to two-dimensional case shown in Figure 17 .This three-dimensional USN will then be defined inside a sphere (related to blue circle in Figure 17 of radius equal to N_L. This sphere was called "general sphere" (GS) and will contain the entire network. We can define a subnet contained in a spherical shell concentric whit GS and whit radius equal to N_d. The area on the surface of this spherical shell, for the case of one uniform USN will be defined by:

$$A_U(N_d) = 4\pi\, N_d^2 \tag{16}$$

This spherical shell will cut a certain number (N_c) of uspheres.If we consider that these uspheres will be divided in half, creating a circular section, we can make the following approximation:

$$A_U(N_d) \cong N_C\; 2\pi\, r_0^2$$
$$A_U(N_d) = N_C\; 2\,\pi\alpha\; r_0^2 \tag{17}$$

Where α is an adjustment factor whose value is slightly larger than the unit. Considering now the distorted network, we will compress a single usphere which is found in the center of the network. We can then assume the radius of the neighboring uspheres will increase, causing an increase in volume and surface area of each network usphere. Generically it is possible to consider that the area of each usphere in the distorted network will increase accordingly to the function $K(N_d)$, where N_d is the distance between the point considered, and the distortion point, in network center.

In this context, the following generic equation, relating the radius of the distorted usphere $r_x(N_d)$ with the original radius can be defined as:

$$r_x^2(N_d) = r_0^2(1 + K(N_d)) \tag{18}$$

We now need to consider the increasing of the USN total volume due to compression of an usphere in its interior. Figure 18 shows the case of the flattened USN network, presented in blue in Figure 17, with one inside usphere being compressed. The uspheres in Figure 18-b increase in size due to two factors: occupation of the space left by the compressed usphere and occupation of the

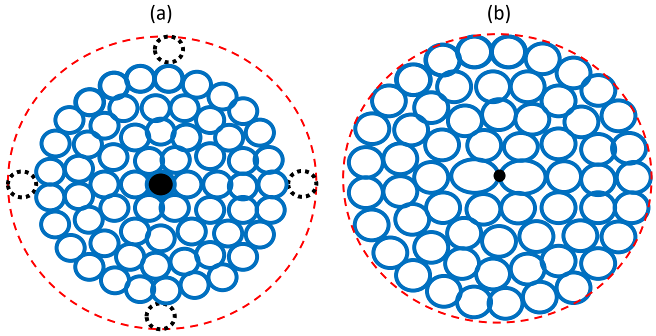

Figure 18:
a) Uniform two-dimensional usphere network,
b) Distorted network The collapse in central usphere (represented in black) generates an increase in the network total area.

For the case of a three-dimensional USN, defined within the GS, we will calculate a surface area (A_D) defined in the distorted network. Considering that the number (N_c) of uspheres that intersects the defined spherical shell will not vary, it can be applied the equation (18) in equation (17), obtaining:

$$A_D(N_d) = N_C\; 2\,\pi\alpha\; r_0^2(1 + K(N_d))$$
$$A_D(N_d) = A_U(N_d)(1 + K(N_d)) \tag{19}$$

Equation 19 indicates that for the distorted USR, the radius increasing leads to an increase on the individual areas of each usphere which is equivalent to the increment observed on the spherical shell distorted area A_D.

If we now take the spherical shell defined by the GS ($N_d = N_L$) applying equation (16) we obtain the value of the total area undistorted in GS (A_{UGS}):

$$A_{UGS} = 4\pi\, N_L^2 \tag{20}$$

Within the analogy shown in Figure 18, suppose that at the distorted three-dimensional USR, the radius of the GS increases by one unit. In this case it is like the collapse of the central usphere generates a new uspheres shell on the three-dimensional network edge.
Thus, applying equation (20), with the N_L value increasing by one unit, the total area of the distorted GS (A_{UGS}) is then given by:

$$A_{DGS} = 4\pi\,(N_L + 1)^2$$
$$A_{DGS} = 4\pi\,(N_L^2 + 2N_L + 1)$$
$$A_{DGS} \cong 4\pi\,(N_L^2 + 2N_L) \tag{21}$$

Applying the equations (20) and (21) in equation (19) the results are the following:

$$A_{DGD} = A_{UGS}(1 + K(N_d))$$
$$4\pi(N_L^2 + 2N_L) = 4\pi\, N_L^2(1 + K(N_L))$$
$$N_L^2(1 + \frac{2}{N_L}) = N_L^2(1 + K(N_L))$$
$$K(N_L) = \frac{2}{N_L} \quad (22)$$

Thus, the increase in radius defined in equation (18) will be given by the following function:

$$r_x^2(N_d) = r_0^2(1 + \frac{2}{N_d})$$
$$r_x(N_d) = r_0\sqrt{(1 + \frac{2}{N_d})} \quad (23)$$

Equation (23) describes the radius increase of each usphere in a uniform network where a single udyhole is being generated for the case in which the final volume of the distorted network increases, similarly to that shown in Figure 18.

Figure 19 shows a comparative graph between equations (14) and (23) where we can observe, that as expected, the increase in radius for the case of equation (23) is much larger than the increase described by equation (14).

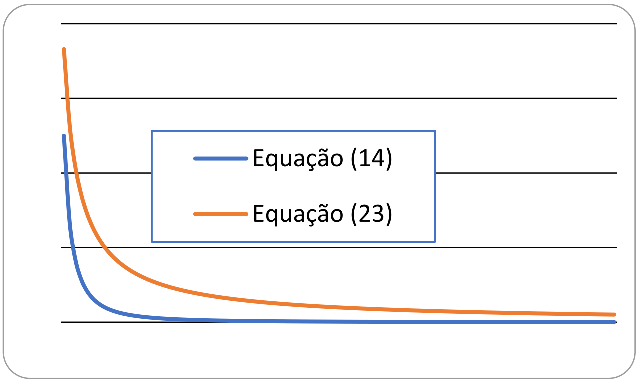

Figure 19: Expansion of the usphere radius in function of its distance from the distortion point.

If we consider that instead of a single udyhole in the distortion point, there are udyholes being formed, we can assume that the factor $K(N_d)$ will be applied times. Thus, the increase in radius described in equation (23) will be achieved by using a $NK(N_d)$ factor. Considering also that each udyhole has a unitary mass (K_{mu}), the total mass associated to the space distortion is given by:

$$M = NK_{mu} \quad (24)$$

Based on equations (23) and (24) the following equation can be defined:

$$r_x(N_d) = r_0\sqrt{(1 + N\frac{2}{N_d})}$$
$$r_x^2(N_d) = r_0^2(1 + \frac{2M}{K_{mu}N_d}) \quad (25)$$

Equation (25) defines how each usphere's radius of a symmetric network varies accordingly to the presence of a mass M at its center.In order to translate the equation (25) accordingly to a metric of non-Euclidean space, we need to consider two ways for calculating the distance in space-time defined in the USN model. The real metric should take into account the effective radius of each network usphere, given by equation (23), while the digital metric is obtained by simply counting of uspheres without worrying about the actual size of each one of them.
Considering the treatment of the space-time in a Minkowski metric, a distance (real metric) in the space-time is given by:

$$da^2 = a_1^2 - a_2^2 - a_3^2 - a_4^2 \quad (26)$$

From equation (12), each usphere's diameter is associated to a Planck distance and the measurement of distances in digital metric assumes the following form:

$$ds^2 = c^2dt^2 - dx^2 - dy^2 - dy^2 \quad (27)$$

Equations (26) and (27) are defined in a context where the distance is related to a real metric, while the distance is related to a digital meter, so that for an undistorted network the two distance values are proportional.

Thus, using equations (12) and (13) in (26) and (27), for a uniform network, we obtain the following linear relation between these two metrics:

$$ds^2 = \frac{\ell_p^2}{r_0^2}da^2 \quad (28)$$

Writing equation (26) for the space (a_1, a_2, a_3, a_4) being defined in terms of spherical coordinates we obtain:

$$da^2 = da_1^2 - dr_R^2 - r_R^2 d\Omega^2 \quad (29)$$

Where represents a defined radius in real metric and $d\Omega^2$ is defined as shown in equation (6).Likewise, equation (27) can be written in spherical coordinates:

$$ds^2 = c^2dt^2 - dr^2 - r^2 d\Omega^2 \quad (30)$$

Where r represents a radius defined in digital metric and ($d\Omega^2$) is defined as shown in equation (6).For a uniform network, the relation between the radius defined by two metrics is given by:

$$r_R = \frac{\ell_p}{r_0}r \quad (31)$$

In case of N udyholes (total mass equal to M) that distorts the network, we can consider that the value da^2 can be calculated by equation (25) applied as follows:

$$da^2(N_d) = da^2(\infty)(1+\frac{2M}{N_d \mathrm{K_{mu}}}) \qquad (32)$$

Where the term $da^2(\infty)$ indicates the metric for an infinite distance from the distortion point, which is equal to the original uncompressed network metric:

$$da^2(\infty) = da_1^2 - dr^2 - r^2 d\Omega^2 \qquad (33)$$

Equation (32) shows that the presence of mass causes a change in the digital metric in the center of the network in which the distances are smaller, because the uspheres radius increase is bigger in this point.

Figure 20 shows again the analogy of a river crossed by rows of different sizes of stones. In Figure 20-a, the blue square represents a river, where in the left margin "stones" are observed, represented in red, they have the original size and in the right margin they are multiplied by a factor b (equal to two in this example). Figure 20-b shows the digital metric in which all the "stones" have the same size. In Figure 20-a, we also observe two green circles that have the same area (X^2) and will be used as objects of analysis. The green circle, on the right on Figure 20-b, will have only ¼ of the original area, because the uspheres of the right margin doubled it size in real metric.

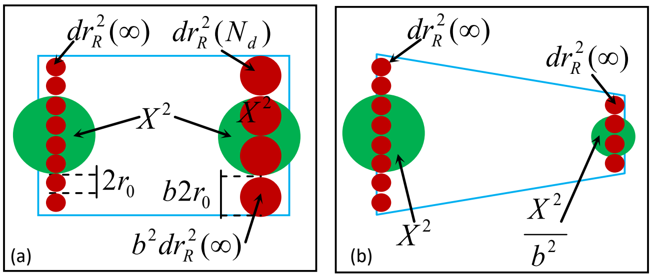

Figure 20: Analogy of a river crossed by rows of stones: a) Real metric; b) Digital metric.

We can see from this example that when a factor b^2 multiplies the value $dr_R^2(\infty)$ in the real metric, the same factor b^2 will divide the value of objects areas (X^2) in the digital metric. Thus, the expansion of uspheres in the real space generates a "shrinking" of distances and areas in digital space.

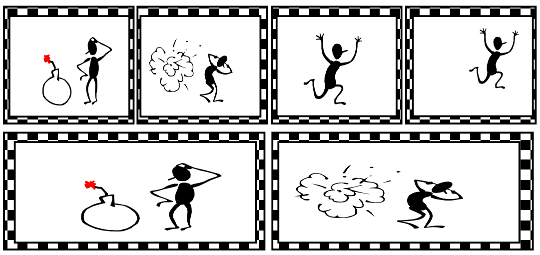

Figure 21: Analogy of a pellicle being "stretched" so that each frame has twice the size.

However, this consideration of "shrinkage" is not valid for the temporal dimension. In order to observe this aspect, let us take an analogy of a movie pellicle where the total time can be associated to the number of slides multiplied by the width (related to the time dimension) of each slide.

In the analogy of Figure 21, suppose that a "time distortion" stretches every frame of the film making it last twice its duration. In this case, for example, a one-hour duration film will be displayed in two hours.

More generally this means that if da^2_1 (which is related to time in the real metric) is multiplied by a certain factor, then the "temporal distance" in digital metric also will be multiplied by the same factor.

In terms of equations, this means that for a factor β that multiplies the space-time real metric, in digital metric, the time will be multiplied by the same factor β and the space will be multiplied by the inverse of factor β. Therefore, considering the relation given by equation (28) we can state that:

$$\beta da_1{}^2(\infty)\frac{\ell_\mathrm{p}{}^2}{r_0^2} = \beta c^2 dt^2(N_d) \qquad (34)$$

$$\beta dr_R^2(\infty)\frac{\ell_\mathrm{p}{}^2}{r_0^2} = \frac{1}{\beta}dr^2(N_d) \qquad (35)$$

It is worth to remember that the angular displacement $d\Omega^2$ defined on a sphere does not vary when the radius of this sphere is multiplied by any non-null factor.
Thus, considering the expansion of an usphere in the point N_d given by a factor β, equation (29) can be written as:

$$\begin{aligned} da^2(N_d) &= \beta(da_1^2(\infty) - dr_R^2(\infty) - r_R^2(N_d)d\Omega^2) \\ da^2(N_d) &= \beta da_1^2(\infty) - \beta dr_R^2(\infty) - r_R^2(N_d)d\Omega^2 \end{aligned} \qquad (36)$$

Applying equation (28) in equation (36) we obtain:

$$ds^2(N_d) = \frac{\ell_\mathrm{p}{}^2}{r_0^2}(\beta da_1^2(\infty) - \beta dr_R^2(\infty) - r_R^2(N_d)d\Omega^2) \qquad (37)$$

Since applying the equations (34) and (35) in equation (37) we obtain:

$$\begin{aligned} ds^2(N_d) &= \beta c^2 dt^2(N_d) - \frac{dr^2(N_d)}{\beta} - r^2(N_d)d\Omega^2 \\ ds^2 &= \beta c^2 dt^2 - \frac{dr^2}{\beta} - r^2 d\Omega^2 \end{aligned} \qquad (38)$$

In order to complete the proposed analysis we must now calculate the factor β to be used in equation (38).Looking again at equation (25) we can consider that this factor is given by:

$$\beta = (1+\frac{2M}{N_d \mathrm{K_{mu}}}) \qquad (39)$$

However, there is a problem associated with the equation (39) application which regards to the parameter N_d. This parameter is related to a distance in the digital metric of the undistorted network, which is directly connected to the real metric. Thus, we need to obtain the factor β based on the observed distances in the digital metric with distorted network, which will be calculated from the example shown in Figure 22.

Figure 22 represents a similar scheme to that shown in Figure 20, but with uspheres areas being represented in a rectangular shape for easy viewing.

Figure 22-a presents a real metric, where the red rectangle represents an undistorted usphere while the blue rectangle represents an amplified usphere due to the distortion of the network. The ratio of the areas in Figure 22-a is obtained based on equation (32).

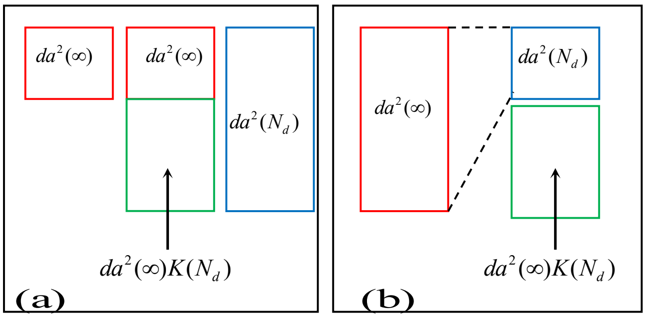

Figure 22: Observation of the variation of the metric in two view points: a) Real metric; b) Digital metric.

In the table shown in Figure 22-b we observe the view of the digital metric where the blue area decreases after being multiplied by a factor $1 / \beta$. Based on Figure 22-b, we can obtain the following equation:

$$da^2(\infty) = da^2(N_d) + da^2(\infty)K(N_d)$$
$$da^2(N_d) = da^2(\infty) - da^2(\infty)K(N_d)$$
$$da^2(N_d) = da^2(\infty)(1 - K(N_d))$$
$$da^2(N_d) = da^2(\infty)(1 - \frac{2M}{N_d \mathrm{K}_{\mathrm{mu}}}) \quad (40)$$

Considering in this case the factor β is defined by:

$$\frac{1}{\beta} da^2(N_d) = da^2(\infty) \quad (41)$$

Applying equation (41) in equation (40) the factor β can be calculated by:

$$\beta = (1 - \frac{2M}{N_d \mathrm{K}_{\mathrm{mu}}}) \quad (42)$$

The parameter N_d used in equation (42) was obtained in the context of the distorted network digital metric, thus being usable by an observer who has access to this metric. Also considering that in the desired point the r value is given by:

$$r = N_d \ell_{\mathrm{p}} \quad (43)$$

Applying equation (43) in (42):

$$\beta = (1 - \frac{2M\ell_{\mathrm{p}}}{r\mathrm{K}_{\mathrm{mu}}}) \quad (44)$$

We can demonstrate that the Planck distance and unitary mass values are defined by the following equation:

$$\ell_{\mathrm{p}} = \sqrt{\frac{\hbar G}{c^3}} \quad (45)$$

$$\mathrm{K}_{\mathrm{mu}} = \sqrt{\frac{\hbar c}{G}} \quad (46)$$

Applying (45) and (46) in (44) we obtain:

$$\beta = (1 - \frac{2M}{r}\sqrt{\frac{\hbar G}{c^3}\frac{G}{\hbar c}})$$
$$\beta = (1 - \frac{2GM}{rc^2}) \quad (47)$$

Finally, applying equation (47) in equation (38) we obtain:

$$ds^2 = (1 - \frac{2GM}{c^2 r})c^2 dt^2 - \frac{dr^2}{1 - \frac{2GM}{c^2 r}} - r^2 d\Omega^2 \quad (48)$$

Where equation (48) is equal to the expression (5), *quod erat demonstrandum.*

5.1. New Interpretation of the Schwarzschild Radius

Within the USN model, the Schwarzschild radius has an interesting interpretation when its value is observed in Planck units and the mass M is distributed along a straight line, as shown in Figure 23.

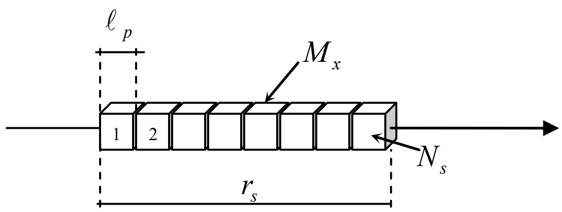

Figure 23: Division of the original mass M in equal "cubes" aligned along a straight line.

In Figure 23 we can observe the number (N_s) of "cubes", in which the mass M was distributed, is given by:

$$N_s = \frac{r_s}{\ell_p} \quad (49)$$

Thus the mass (M_x) of each "cube" shown in Figure 23 will be given by:

$$M_x = \frac{M}{N_s} \quad (50)$$

Applying equations (49) and (45) in the equation (50) we obtain:

$$M_x = \frac{M}{r_s}\sqrt{\frac{\hbar G}{c^3}} \quad (51)$$

Applying equation (8) which defines the Schwarzschild radius in equation (51) we obtain:

$$M_x = \frac{M}{2GM}\frac{c^2}{}\sqrt{\frac{\hbar G}{c^3}}$$

$$M_x = \frac{1}{2}\sqrt{\frac{\hbar c}{G}} = \frac{1}{2}\mathrm{K}_{mu} \quad (52)$$

Thus each "cube" will have half of a unitary mass value, in other words, half the mass of an udaynahole.

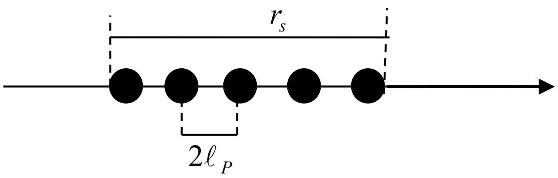

Figure 24: Alignment of udyholes in a straight line.

This means that if the original mass M is divided into a line of udaynaholes, with the distance between their centers equal to twice the Planck distance, its length of this line will be equal to the Schwarzschild radius, as shown in Figure 24.

Figure 25 shows an analogy with a two-dimensional surface formed by an elastic membrane, in which some colored concentric circles were painted. Considering that this membrane is fixed on a flat surface with a hole in the center, the inclusion of an udyhole would be equivalent to pulling a circular area of the membrane into the hole.

We can see in Figure 25 that each added udyhole "sucks" one of the colored rings, and thus, the total collapsed area will be proportional to the squared number of udyholes. For the three-dimensional case, the accumulation of N dyholes in the same position will collapse a volume proportional to the value of N^3.

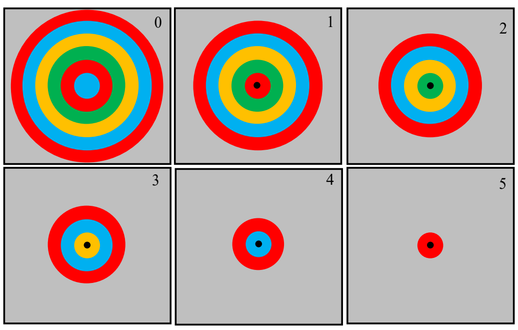

Figure 25: Udyholes overlapping on an elastic surface. The number in each table indicates how many udyholes are overlapped on each event.Thus dividing the mass M in N udyholes of unitary mass, the distance obtained by aligning them as illustrated in Figure 26, will define the total radius of the compressed sphere (equal to $2\ell_p N$) which is the Schwarzschild radius itself.

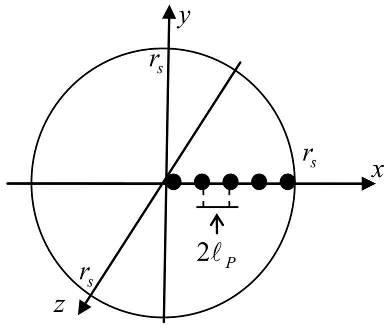

Figure 26: Sphere with Schwarzschild radius in which a set of udyholes is aligned on an axis

6. Deduction of the Newton's law

As mentioned in previous section we consider the USN total volume does not change when udyholes are generated in its interior and equations (14) and (15) are valid. In this case, we can consider that the collapse of an usphere, as shown in Figure 16 generates radial force fields that propagate through the network. Taking the forces in any radial direction we will notice that the force that compresses an usphere in the center of the network will propagate from a usphere to another, as shown in Figure 27, through a series of pairs of action forces (blue in the figure) and reaction (in red) that are decreasing in intensity, tending to null in the end of the USN.

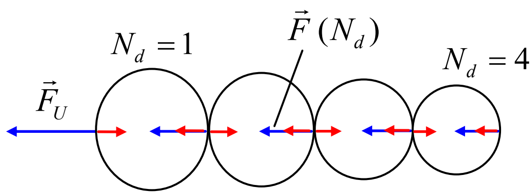

Figure 27: Forces that arise in a given direction when the usphere is compressed.In this case equation (14) can generate the following simplified expression:

$$r_x(N_d) = r_0\left(1 + \frac{1}{N_d^2}\right) \quad (53)$$

Based on equation (53) and considering the force applied on the uspheres has an elastic behavior ($F = Kx$), the module of the forces shown in blue in Figure 24 will be modeled by the following equation:

$$F(N_d) = F_U \frac{1}{N_d^2} \quad (54)$$

Where F_U is a unitary force. If we have now, in the same USN two udyholes separated by a distance d given in meters ($d = \ell_p N_d$), each one of them will generate an equivalent force on the other, as defined by equation (54), which varies in function of the distance d accordingly to the following expression:

$$F = F_U \frac{1}{(d/\ell_p)^2} \quad (55)$$

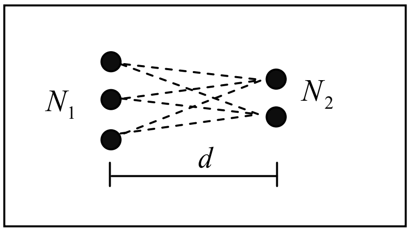

Figure 28: Two groups of udyholes interacting from a distance *d*.Now considering a more general case, in which the first point, we have N_1 udyholes and in the second point N_2 udyholes, as shown in Figure 28. The force arising between the two groups of udyholes is given by:

$$F = N_1 N_2 F_U \frac{\ell_p^2}{d^2} \quad (56)$$

Considering that each udyhole has a unitary mass defined as in the equation (24), the equation (56) can be written as follows:

$$F = F_U \frac{M_1}{K_{mu}} \frac{M_2}{K_{mu}} \frac{\ell_p^2}{d^2} \quad (57)$$

Applying the equations (45) and (46) in (57) we obtain:

$$F = F_U \frac{G}{\hbar c} \frac{\hbar G}{c^3} \frac{M_1 M_2}{d^2}$$

$$F = F_U \frac{G^2}{c^4} \frac{M_1 M_2}{d^2} \quad (58)$$

We can show that in the units system defined in the USN model, the force can be calculated by:

$$F_U = \frac{c^4}{G} \quad (59)$$

Applying equation (59) in (58) we obtain:

$$F = G \frac{M_1 M_2}{d^2} \quad (60)$$

Therefore, the equation (60) is equal to the gravitation law defined by Isaac Newton.

7. Conclusion

Besides providing a new way to display to non-Euclidean spaces, the Ulianov Sphere Network model presented in this article allowed the calculation of the formula which defines the Schwarzschild metric and the deduction of Newton's law for gravitation.

The key point of the USN model can be seen in Figure 15, where the "space squares" expand due to the presence of udyholes generating an opposite view of the traditional model defined by Einstein in the GRT context where the presence of matter has the effect of shrinking the "space squares ".

Although the USN model at first presents the same results already obtained by GRT, we believe that the complexity of calculation is much smaller, which should make the usage of the USN model interesting in terms of both analytical studies and in digital simulations.

Please notice that the USN model at first is not directly related to the operation of our universe. However, the results obtained by applying the USN model point to the possibility that space-time in our universe may be in fact "sustained" by some kind of hyper-dimensional network, resembling the concept of ether, which was virtually eliminated in the GRT context.

Thus, the author believes the USN model can be also a source of inspiration for theoretical physicists and represents another step towards a more complete model of the universe [15-32].

NOTE: The Ulianov Sphere Network is part of a larger picture of theories developed by the author, called Ulianov Theory (UT).

References

1. Eves, H. W. (2004). Introdução à história da matemática (p. 77). Campinas: Unicamp.
2. Boyer, Carl. (1974). História da Matemática, Edgard Blücher.
3. May, K. O., & Gauss, C. F. (1972). Dictionary of Scientific Biography (Vol. 5, pp. 298–315). New York: Scribner.
4. Bao, D., Chern, S. S., & Shen, Z. (2000). An introduction to Riemann-Finsler geometry (Vol. 200). Springer Science & Business Media.
5. Ziegler, G. e Aigner, M. (2002). As provas estão no Livro, Ed. Edgard Blücher Ltda.
6. Poincaré, H. (1985). O valor da ciência, Tradução: Maria H. F. Martins. 2a ed. Rio de Janeiro-RJ: Contraponto.
7. Einstein, A. (1920). Relativity: The Special and General Theory. H. Holt and company, NY
8. Krall, G. (1953). Tullio Levi-Cività e la relatività.
9. Corry, L. (1998). The influence of David Hilbert and Hermann Minkowski on Einstein's views over the interrelation between physics and mathematics. Endeavour, 22(3), 95-97.
10. Do Carmo, M. P. (2010). Geometria diferencial de curvas e superfícies. Sociedade Brasileira de Matemática.
11. Adler, R., Bazin, M., Schiffer, M., & Romain, J. E. (1965). Introduction to general relativity.
12. Frolov, V., & Novikov, I. (2012). Black hole physics: Basic concepts and new developments (Vol. 96). Springer Science & Business Media.
13. Klein Martin, J. (1962). Max Planck and the beginning of the quantum theory. Archive for History of Exact Science, 1(5), 459-479.
14. Ulianov, P. Y. (2012). "Small Bang Creating a Universe from Nothing." https://vixra.org/abs/1201.0109
15. Ulianov, P. Y. (2015). Freeman AG Small Bang Model. A New Model to Explain the Origin of Our Universe. Global Journal of Physics, 3(1). https://vixra.org/abs/1211.0157
16. Freeman A. G., Ulianov P. Y. (2011) "The Small Bang

Model - A New Explanation for Dark Matter Based on Antimatter Super Massive Black Holes." http://vixra.org/abs/1211.0157
17. Ulianov, P. Y. (2010). "Ulianov String Theory A new representation for fundamental particles." https://www.academia.edu/download/89325911/1201.0101v1.pdf
18. Ulianov, P. Y. One Clue to the Proton Size Puzzle: The Emergence of the Electron Membrane Paradigm." https://vixra.org/abs/1302.0026
19. Ulianov, P. Y. (2012) "Explaining the Variation of the Proton Radius in Experiments with Muonic Hydrogen." https://vixra.org/abs/1201.0099
20. Ulianov, P. Y. Rotating the Einstein's light clock, to explain the Witte Effect. A basis to make the LIGO experiment work." https://vixra.org/abs/1302.0134
21. Policarpo, Y. Ulianov: Explaining the Variation of the Proton Radius in Experiments with Muonic Hydrogen. January 2012." https://vixra.org/abs/1201.0099
22. Ulianov, P. Y. (2012). "A New Digital Complex Model of Time." https://vixra.org/abs/1201.0102
23. Ulianov, P. Y. (2013). "Spacetime Dipole Waves Pressure and Elemental Particles." https://vixra.org/abs/1306.0222
24. Ulianov, P. Y. Spacetime dipole wave pressure and black holes a new way to obtain the Schwarzschild metric, without using general relativity field equations. Asian Journal of Mathematics and Physics, 2013.
25. Ulianov, P. Y. An alternative to the Higgs field mass generation mechanism based on a dipole wave pressure model. Asian Journal of Mathematics and Physics, 2013.
26. Ulianov, P. Y. (2016). Breaking the Paradigm of Negative Mass: Why Newton's Second Law Needs to Be Modified to Enable Newton's Gravitational Law to Deal with Antimatter. Global Journal of Physics Vol, 4(1).
27. Ulianov, P. Y., & Negreiros, J. P. (2015). Does the value of Planck time vary in a Black Hole Event Horizon? A new way to unify General Relativity and Quantum Mechanics. Global Journal of Physics, 3(1), 165-171.
28. Ulianov, P. Y. An alternative to the Higgs field mass generation mechanism based on a dipole wave pressure model. Asian Journal of Mathematics and Physics, 2013. https://vixra.org/pdf/2308.0200v1.pdf
29. Ulianov, P. Y. (2023). "Ulianov Perfect Liquid Model Explaining why Matter Repels Antimatter." https://vixra.org/pdf/2308.0199v1.pdf
30. Ulianov, P. Y., Mei, X., & Yu, P. (2016). Was LIGO's Gravitational Wave Detection a False Alarm?. Journal of Modern Physics, 7(14), 1845. https://www.scirp.org/html/1-7502879_71246.htm
31. Mei, X., Huang, Z., Ulianov, P. Y., & Yu, P. (2016). LIGO Experiments Cannot Detect Gravitational Waves by Using Laser Michelson Interferometers—Light's Wavelength and Speed Change Simultaneously When Gravitational Waves Exist Which Make the Detections of Gravitational Waves Impossible for LIGO Experiments. Journal of Modern Physics, 7(13), 1749-1761. https://www.scirp.org/journal/paperinformation.aspx?paperid=70953
32. Ulianov, P. Y. (2016). How Can We Observe Waves Without Seeing the Ocean? Witte-Ulianov Time Interferometer: A Gravitational-Wave Detector without Low Range Frequency Limitation. Global Journal of Physics, 4(2), 281-300. https://vixra.org/abs/2308.0042